Int J Appl Earth Obs Geoinformation 69 (2018) 13–26

Contents lists available at ScienceDirect

Int J Appl Earth Obs Geoinformation

journal homepage: www.elsevier.com/locate/jag

Application and analysis of geodetic protocols for monitoring subsidence phenomena along on-shore hydrocarbon reservoirs

Antonio Montuori[a,*], Letizia Anderlini[a], Mimmo Palano[a], Matteo Albano[a], Giuseppe Pezzo[a], Ilaria Antoncecchi[b], Claudio Chiarabba[a], Enrico Serpelloni[a], Salvatore Stramondo[a]

[a] Istituto Nazionale di Geofisica e Vulcanologia (INGV), Italy
[b] Ministero per lo Sviluppo Economico (MISE), Direzione Generale per la Sicurezza anche Ambientale delle Attività Minerarie ed Energetiche – Ufficio Nazionale Minerario per gli Idrocarburi e le Georisorse (DGS-UNMIG), Italy

ARTICLE INFO

Keywords:
GPS
Multi-temporal DInSAR
Geodetic protocols
Subsidence
Hydrocarbon exploitation

ABSTRACT

In this study, we tested the "land-subsidence monitoring guidelines" proposed by the Italian Ministry of Economic Development (MISE), to study ground deformations along on-shore hydrocarbon reservoirs. We propose protocols that include the joint use of Global Positioning System (GPS) and multi-temporal Differential Interferometric Synthetic Aperture Radar (DInSAR) techniques, for a twofold purpose: a) monitoring land subsidence phenomena along selected areas after defining the background of ground deformations; b) analyzing possible relationships between hydrocarbon exploitation and anomalous deformation patterns. Experimental results, gathered along the Ravenna coastline (northern Italy) and in the southeastern Sicily (southern Italy), show wide areas of subsidence mainly related to natural and anthropogenic processes. Moreover, ground deformations retrieved through multi-temporal DInSAR time series exhibit low sensitivity as well as poor spatial and temporal correlation with hydrocarbon exploitation activities. Results allow evaluating the advantages and limitations of proposed protocols, to improve the techniques and security standards established by MISE guidelines for monitoring on-shore hydrocarbon reservoirs.

1. Introduction

Land subsidence represents a relevant issue that affects highly developed urban and industrialized areas worldwide, especially those located along the coasts (Antonioli et al., 2017). Possible causes of subsidence processes can be listed as follows: a) natural factors, e.g., tectonic activity, self-weight consolidation of recent sedimentary deposits, oxidation and shrinkage of organic soils (Dokka, 2006; Galloway et al., 1999; Heywood and Pope, 2009); b) anthropogenic processes, e.g., groundwater pumping (Amelung et al., 1999; Bell et al., 2008; Bonì et al., 2015; Galloway and Hoffmann, 2007; Raspini et al., 2013; Taniguchi et al., 2009), urban development (Polcari et al., 2014; Stramondo et al., 2008) and hydrocarbon exploitation (Carbognin et al., 1984; Gambolati et al., 1991; Teatini et al., 2006).

Either natural or anthropogenic ground subsidence may severely affect the environment and the population with dangerous consequences, such as the malfunctioning or collapse of buildings, sinkholes, changes of watercourses, flooding, retreat of coastlines and relative-sea level rise (e.g., Antonioli et al., 2017; Modoni et al., 2013), induced seismicity (Keranen et al., 2014). Natural phenomena, such as thermal and tectonic processes, contribute to induce subsidence with rates of a few millimeters per year. Anthropogenic activities, such as the exploitation of aquifers, are responsible for the largest subsidence contribution with maximum rates of several centimeters per year (e.g., Albano et al., 2016; Bonì et al., 2015; Chaussard et al., 2014; Stramondo et al., 2007; Serpelloni et al., 2013). In addition, the hydrocarbon extraction from crustal reservoirs may accelerate the subsidence process, with rates up to some tens of millimeters per year (Allison et al., 2014; Kolker et al., 2011). Consequently, a proper understanding of the subsidence mechanism is essential to calibrate protocols and best practices for monitoring natural and anthropogenic phenomena, with the aim to reduce the risk for infrastructures, economies, natural environments and human life.

Focusing on subsidence processes associated with hydrocarbon exploitation, the Italian Ministry of Economic Development (hereinafter MISE) has defined general guidelines to monitor production activities in areas with high seismic and hydrogeological risk (Ministero dello Sviluppo Economico, DGS-UNMIG, 2014). Such guidelines describe best practices and protocols for the management and monitoring of anthropogenic activities, particularly focused on induced seismicity,

* Corresponding author.
E-mail address: antonio.montuori@ingv.it (A. Montuori).

https://doi.org/10.1016/j.jag.2018.02.011
Received 23 November 2017; Received in revised form 9 February 2018; Accepted 21 February 2018

ground deformation and pore pressure changes related to hydrocarbon exploitation. One of the main goals of these general guidelines was to establish procedures to analyze the spatial and temporal evolution of environmental parameters, as well as their possible correlations with underground anthropogenic activities. This analysis would allow defining risk mitigation plans for the safety of people, environment and industrial facilities.

In this study, we test these guidelines on some pilot areas to verify how far they can be generalized and consolidated in a larger variety of cases. Along with this rationale, we applied and discussed a land-subsidence monitoring methodology to on-shore hydrocarbon reservoirs. In detail, we jointly use Global Positioning System (GPS) and Differential Interferometric Synthetic Aperture Radar (DInSAR) techniques, which are both well suited for monitoring anthropogenic and/or natural subsidence phenomena (Bamler and Hartl, 1998; Guglielmino et al., 2011; Svigkas et al., 2016; Vollrath et al., 2017; Zhou et al., 2009). Indeed, GPS data provide punctual precise measurements of 3-dimensional (3D) ground deformation fields, with millimeter-level accuracy for the linear long-term rates. The high frequency sampling (usually every 30 s) guarantees a time-continuous monitoring, capable to identify short- and long-term ground displacements. In addition, multi-temporal DInSAR techniques provide time-series of 1D-displacement measurements along the sensor line of sight (LOS), with sparse temporal sampling (revisit time from few days to few weeks), dense spatial sampling, large coverage and high spatial resolution. Hence, they are able to capture signals related with both local and larger-scale phenomena. The combination and integration of the two techniques allow providing a complete description of the ground deformation for the temporal and spatial scales of our problem.

Here, we present results achieved for two selected pilot areas: the Ravenna coastal area (northern Italy) and the southeastern Sicily (southern Italy). These areas exhibit subsidence signals of about several mm/yr (e.g., Devoti et al., 2011; Serpelloni et al., 2013).

The final objectives of this study are:

- The application and testing of geodetic protocols to describe, characterize and monitor local subsidence along on-shore hydrocarbon reservoirs, identifying the most critical areas requiring additional monitoring activities;
- The definition of reference background settings for the multi-temporal and multi-spatial evolution of ground deformations along selected test areas;
- The analysis of possible temporal and spatial relationships between hydrocarbon exploitation activities and surface deformation measurements;
- The evaluation of advantages and limitations of the proposed approach, hence providing feedbacks to improve guidelines established by MISE.

2. Pilot areas

In this section, we describe the pilot areas in terms of geological and tectonic settings as well as natural and anthropogenic activities. Regional information about seismic, tectonic and geological settings have been provided through different sources, such as the Italian parametric and instrumental seismic database (ISIDe), the Italian Seismic Bulletin, the Catalogue of Italian Seismicity, the Database of seismogenic sources, the Italian Accelerometric Archive (ITACA).

2.1. Ravenna coastal area

The Ravenna coastal area (Fig. 1a) is a Quaternary sedimentary basin bounded to the SW and North by the northern Apennines and the southern Alps, respectively (Doglioni, 1993).

Buried under the thick cover of sediments of the Po Plain, the Apennines accretionary wedge is defined by seismic and well data (e.g., Pieri and Groppi, 1981). The wedge consists of three arcuate thrust systems, whose easternmost arc is the active Ferrara-Romagna one (Fig. 1a). These systems are delimited externally by thrust faults, which separate them from the Pedealpine monocline. The structure of the Ferrara-Romagna arc can be subdivided into three second-order features, i.e., Ferrara, Romagna and, more to the East, Adriatic folds (Fig. 1a). Moving SE-ward, the prolongation of the Apennine thrust front in the central Adriatic Sea is less evident (Scrocca et al., 2007).

Since Lower Miocene, the Apennines chain has been characterized by an eastward migration of contemporaneous, co-axial, coupled processes, i.e., compression in the foreland, and extension in the hinterland (e.g., Faccenna et al., 2003; Malinverno and Ryan, 1986). This migration produced a zone of active sedimentation above the deforming accretionary wedge in the western part of the Apennines, and a thinned crust in the eastern side. These processes are still ongoing, as demonstrated by crustal stress (Montone and Mariucci, 2016) and geodetic strain (e.g., Anderlini et al., 2016; Bennett et al., 2012; Serpelloni et al., 2005) measurements. They generate active compression in the present-day foreland (i.e., Adriatic coast and off-shore), and active extension along the axial culmination of the Apennines. This activity is clearly highlighted by the seismicity distribution with many strong ($M > 6$) damaging earthquakes occurred in the last 40 years, e.g., Norcia 1979, Colfiorito 1997, L'Aquila 2009, Emilia 2012 and Central Italy seismic sequence 2016 (DISS Working Group, 2015; Pondrelli et al., 2006, see Fig. 1a).

Within this complex seismotectonic framework, intensive groundwater pumping and hydrocarbon exploitation activities characterized the Ravenna coastal area in the last 40 years (Chahoud and Zavatti, 1999; Regione Emilia-Romagna and ENI-AGIP, 1998; Teatini et al., 2006). A monitoring network of wells, deployed along the region since the middle of 1970s, demonstrated the close relationship between land settlement and groundwater withdrawal. Maximum piezometric decline (up to 40 m) and largest settlement rates (up to 110 mm/yr) were recorded between 1972 and 1973 (Carbognin et al., 1978). Starting from the '80s, the piezometric measurements revealed a significant decrease of subsidence rate (Gambolati et al., 1999). Nevertheless, a residual land settlement was measured all over the region, due to the delayed aquitard consolidation (Teatini et al., 2006).

The study area is also characterized by many hydrocarbon reservoirs (see Fig. 2a). They were generated along the North African continental margin during the Mesozoic and the lower Paleogene, where the continental sedimentation was mainly made by carbonates (Casero and Bigi, 2013). The flexural history of Adriatic lithosphere was the main factor responsible for the generation and accumulation of biogenic/thermogenic hydrocarbons (Casero, 2004). Most of the Italian gas production comes from the Northern Adriatic Sea. The older source is thermogenic gas-prone, the younger source is biogenic gas one. The latter is mostly located in the outer Plio-Pleistocene foredeep domain, which characterizes the eastern Po Plain and Northern Adriatic Sea (Bertello et al., 2010). Nowadays, the study region hosts the most important Italian gas fields, explored since 1950 (Fig. 2a).

2.2. South-eastern Sicily

The geological-structural setting of SE Sicily is part of the complex tectonic features of the Mediterranean basin, dominated by the Neogene-Quaternary convergence between Nubia and Eurasia plates (Faccenna et al., 2001). The Hyblean Foreland (Fig. 1b) mostly represents the investigated area. It consists of an isolated and elevated fore-bulge structure, formed since the early Miocene by bending of the foreland lithosphere beneath the load of the advancing Maghrebian Chain (Billi et al., 2006). The autochthonous sedimentary wedge (about 7 km thick) consists of Triassic to Pleistocene carbonate succession, with intercalated submarine hydro-volcanoclastic units and minor lava flows (Grasso et al., 2004). A major N-S oriented, 70 km long, shear zone, known as Scicli line or Scicli-Ragusa Fault System (SRFS in

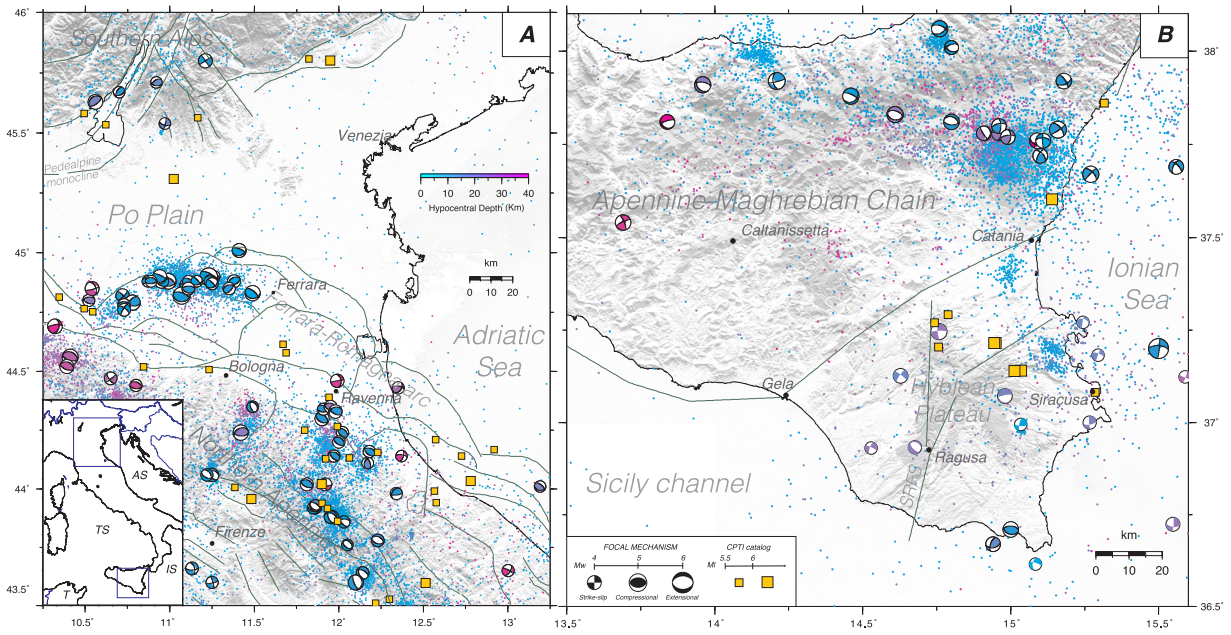

Fig. 1. Seismotectonic setting of (a) the on-shore Po Plain region and (b) the SE Sicily sector. Green lines indicate main active fault systems, where depth-colored beachballs refer to focal mechanisms of earthquakes with M > 3.5 (Musumeci et al., 2014; Pondrelli et al., 2006). Yellow squares indicate strong historical earthquakes from CPTI15 catalog (Rovida et al., 2016) starting from A.D. 1000. Inset acronyms, T: Tunisia; TS: Tyrrhenian Sea; AS: Adriatic Sea; IS: Ionian Sea. SRFS stands for Scicli-Ragusa Fault System. (For interpretation of the references to colour in this figure legend, the reader is referred to the web version of this article.)

Fig. 1b; Ghisetti and Vezzani, 1980; Grasso and Reuther, 1988), cuts the Hyblean Plateau. It extends from the frontal thrust belt of the Apennine-Maghrebian Chain (in the north, Fig. 1b) to the southern off-shore. It consists of three NS-trending main fault segments and second-order structures, with NE-SW en-echelon arrangement that accommodate the shear deformation (Catalano et al., 2010). Since about 0.85 Myr, left-lateral motions have partially reactivated the northern SRFS segments (Catalano et al., 2008).

The investigated area experienced some destructive events, such as the 1169 and 1693 earthquakes (MCS intensities of XI, with estimated magnitudes of about 7 or higher; Boschi et al., 2000), and more recently, a ML = 5.4 earthquake in 1990, about 10 km in the Ionian offshore (Amato et al., 1995). Instrumental seismicity is confined in a depth interval of 15–25 km and is concentrated along the northern segment of SRFS, on the eastern side of the Plateau. Focal mechanism solutions and slip kinematics of Holocenic faults evidenced that the area is currently subject to a general strike-slip faulting regime. Its maximum horizontal stress axis is NW-SE to NNW-SSE oriented, in agreement with the Nubia-Eurasia convergence direction (Mastrolembo Ventura et al., 2014; Musumeci et al., 2014).

Groundwater pumping activities from subsurface aquifers characterized the interested area, and represented the major source for municipal-industrial water supply of local towns. Shallow aquifers (depth > 10 m) develop within alluvial deposits, and therefore are concentrated along the main rivers and drainage networks. Conversely, deeper aquifers (depth > 150 m) develop in calcareous deposits (Aureli et al., 1987), which outcrop extensively over the investigated area. Starting from 1980s, the overexploitation of the aquifer system produced a decline of the hydraulic head, up to 100 m (Aureli et al., 1987).

The investigated area was further interested by the exploitation of surficial asphalt deposits during the 19th and early 20th centuries.

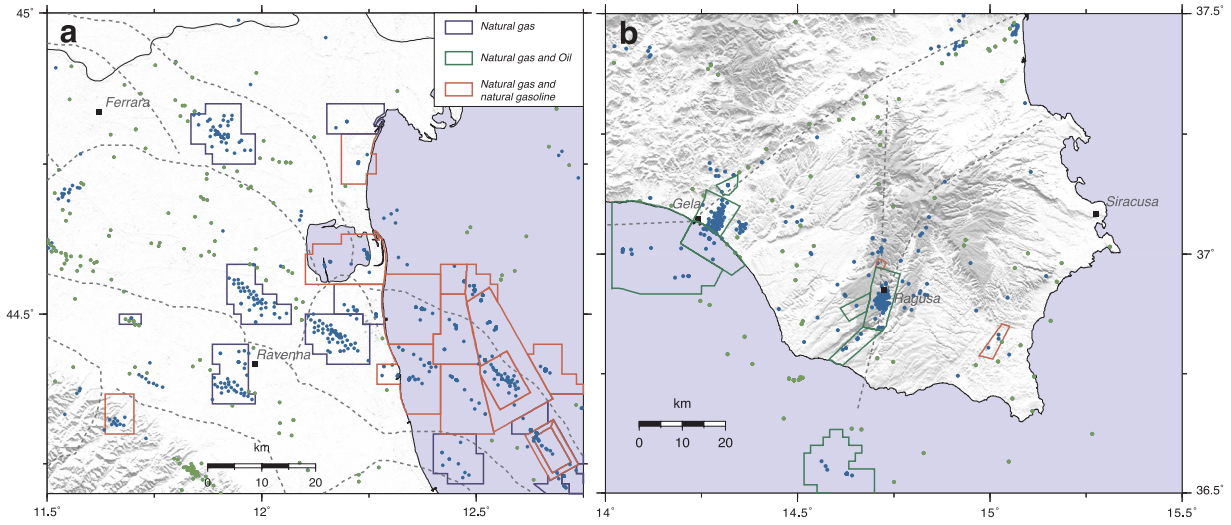

Fig. 2. Reservoirs located along (a) Ravenna and (b) SE Sicily coasts, indicating their specific oil/gas production. Existing and available wells are shown in blue and green colors, respectively. Main fault systems are plotted as dashed lines. (For interpretation of the references to colour in this figure legend, the reader is referred to the web version of this article.)

Several shallow wells were drilled before the World War II. In detail, the first well for oil production was drilled in 1953 on the western sector of the Hyblean Plateau (Fig. 2b, Granath and Casero, 2004). Onshore exploration peaked in 1959 and tapered off in 1970 in response to several factors, i.e., the low quality of discovered oil, the complex geology, the low prices of the oil, and the approval of a restricted Sicilian hydrocarbon law. After 1969, part of the Sicilian offshore was opened to exploration activities (Granath and Casero, 2004). The price boom in the late 1970s and the advent of digital seismic acquisition spurred the activity of hydrocarbon exploitation, and heavy crude oil was discovered at some off-shore sites. Since 1992, the activity has been decreased both on-shore and off-shore. However, in the last years, some new parts of the off-shore have been subjected to further exploration and several operators hold new permissions.

3. Geodetic protocols

In this section, we describe the geodetic protocols adopted for the analysis of subsidence phenomena, in terms of data collection and processing techniques. They include the multi-temporal processing of geodetic data from GPS stations and space-borne SAR sensors, properly integrated according to the following scheme (Fig. 3).

First, we have collected long-term GPS data from continuous networks deployed along the pilot areas. Hence, we have applied consolidated procedures to retrieve long-term ground displacement rates in a well-defined terrestrial reference frame. Afterwards, we have processed available SAR images for the pilot areas through multi-temporal DInSAR techniques, to retrieve time-series of ground deformations and mean surface velocities.

Subsequently, we have integrated GPS and multi-temporal DInSAR measurements according to the procedure described in Zebker et al. (1994). The latter allows tying SAR-based products to the terrestrial GPS reference frame, removing potential residual orbital errors likely present in the multi-temporal DInSAR velocity maps. The integrated multi-temporal GPS and DInSAR products provide a reference background for the analysis of main subsidence and ground deformation patterns, at both local and regional-scales. This is due to the different resolution and sampling capabilities of the two geodetic techniques.

Following the first two processing steps, we have compared multi-temporal DInSAR velocity maps to continuous GPS velocities for validation purposes. Finally, we have compared the ground displacement time series to available hydrocarbon production data, in order to analyze possible spatial and temporal relationships between exploitation activities and surface deformation processes in the two pilot areas.

3.1. GPS data collection and processing

GPS observations cover the time interval 1995–2016, with the largest contributions available after 2005 and at least 2.5 years of continuous observations. They have been collected from:

- The National Integrated GPS Network (RING) deployed by the National Institute of Geophysics and Volcanology (INGV) for crustal deformation monitoring (INGV RING Working Group, 2016);
- GPS stations installed by other public and private institutions (e.g., administrations, universities, private companies) for topographic applications (e.g., mapping and cadastral purposes), as well as local/regional monitoring and positioning;
- Survey-mode GPS measurements collected during several weekly-long campaigns.

We have processed GPS data using the GAMIT/GLOBK 10.6 software package (Herring et al., 2010) adopting the strategy described in Serpelloni et al. (2013). To improve the network configuration and tie the regional measurements to an external global reference frame, we have further collected GPS data from the continuous global tracking stations of IGS (Dow et al., 2009) and EUREF (Beutler et al., 2008) permanent networks. Finally, we have combined all GAMIT solutions and their full covariance matrices, to estimate a consistent set of positions and velocities in a fixed Eurasian reference frame (Cannavò and Palano, 2015).

3.2. SAR data collection and processing

We have acquired 374 SAR images from C-band ERS-1/2 and Envisat SAR missions, covering the time period of 1992–2000 and 2003–2010, respectively. We have collected SAR dataset in Single Look Complex (SLC) format (i.e., high resolution) along both ascending and descending orbits, thus providing a total number of 4 SAR datasets for each case study. All the features of the SAR datasets are listed in Table 1 (see supplementary material).

We have processed each SAR dataset through the multi-temporal DInSAR technique based on the Small Baseline Subsets (SBAS) approach (Berardino et al., 2002), to retrieve ground displacements and mean surface velocities along the satellite LOS. The SBAS approach uses differential interferograms, obtained from coupled SAR images along nearby orbits (i.e., spatial baselines) and with low revisit time (i.e., temporal baselines), to retrieve time series of surface displacement in spite of a reduced SAR pixel resolution (Berardino et al., 2002). Here, we have adopted the SBAS approach through the SARscape© module of ENVI-IDL software, whose setup values are listed in Table 2 (see supplementary material). The latter have been chosen to reduce both speckle noise in SLC SAR imagery and phase artifacts related to spatial/temporal decorrelation issues. They ensure a reliable stack of interferometric pairs with a large density of points in each SAR imagery.

3.3. SAR and GPS integration

Following the multi-temporal DInSAR processing, we have used GPS surface velocity estimations to improve SAR-based products, according to the methodology described in Zebker et al. (1994). The procedure allows tying SAR-based velocities to the ground-based GPS terrestrial reference frame, estimating a planar signal that represents residual orbital errors within multi-temporal DInSAR maps. In detail, for each SAR-based dataset, we have performed the following steps:

- We have defined a set of GPS velocities, obtained from stations with at least 6 years of observations and located close enough to SAR

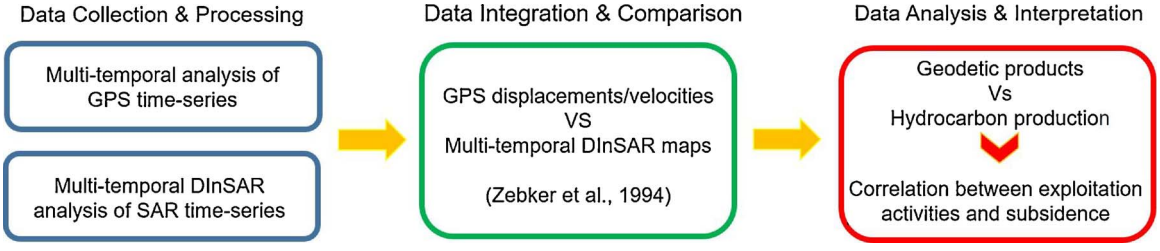

Fig. 3. Block scheme for the proposed geodetic protocol.

pixels. This choice allows assuming that both techniques measure the same deformation signal. Moreover, the selected GPS stations should be distributed as much as uniformly across the SAR-based velocity map;
- We have projected the 3 components (East, North and Up) of GPS velocities along the SAR sensor LOS, assuming that the long-term rates did not change over time;
- We have evaluated mean and median values of SAR-based ground velocities in the surroundings of each GPS station;
- We have corrected the misfits between GPS and surrounding DInSAR velocities, estimating a three-parameter planar ramp by means of a linear least square inversion. The ramp allows correcting the SAR-based velocity maps, when possible.

4. Experimental results

In this section, we present some results obtained from the application of the above-described geodetic protocols in the pilot areas of Ravenna coastline and SE Sicily.

4.1. Ravenna coastal area

Fig. 4 shows the GPS velocity (in the Eurasian-fixed reference frame) and strain-rate fields in the Ravenna coastal area. GPS horizontal velocities depict a crustal deformation field with velocity vectors oriented along N-S and NNE-SSW directions (see Fig. 4a), in agreement with the overall counterclockwise rotation of the Adriatic microplate (Anderlini et al., 2016; Serpelloni et al., 2016). The horizontal strain rate field has been computed on a regular grid (Fig. 4b) using the method of Tape et al. (2009). It shows both compressive (red arrows) and extensional (blue arrows) processes, with rates up to 30–40 nanostrain/yr. GPS measurements also provide a vertical velocity field showing an overall subsidence rate of 1–2 mm/yr for most of the Po Plain, with values higher than 3 mm/yr along the Adriatic coast (see Fig. 4a). Finally, positive velocity values (uplift) characterize part of the Apennines chain (Fig. 4a), representing a geodynamic and tectonic signal (Faccenna et al., 2014).

Fig. 5 shows the SAR-based LOS mean surface velocity maps of Ravenna coastal area, gathered through ERS and Envisat datasets along both acquisition orbits, following the GPS-SAR integration procedure described in Section 3.3. We observe negative surface velocities (i.e., points moving away from the satellite) up to 12 mm/yr with mean subsidence rates between 2.5–5 mm/yr in the time period 1992–2000 (see ERS-1/2 results along ascending and descending orbits in Fig. 5a–c, respectively). Similar results have been obtained for the Envisat dataset acquired along both orbits in the period 2003–2010 (see Fig. 5b–d). Our results show the highest subsidence rates along the coastline and near the major urban settlements, with values ranging between 5 and 10 mm/yr (see Fig. 5). Moreover, we observe some uplift phenomena, mainly located along the Apennines (see red patches in Fig. 5) in agreement with GPS-based vertical velocities (Fig. 4a).

To study the spatial consistency of GPS and SAR-based experimental results, we have compared multi-temporal DInSAR and GPS velocity fields. The selected GPS velocities, projected along the SAR sensor LOS, are shown as colored circles in Fig. 5 (with the same color-palette of DInSAR velocities). The root mean square error (RMSE) values between GPS and DInSAR measurements are equal to: (i) 0.3 mm/yr and 1.7 mm/yr for the ERS ascending and descending dataset, respectively; (ii) 0.2 mm/yr and 0.6 mm/yr for the Envisat ascending and descending dataset, respectively. These results highlight the good agreement between multi-temporal DInSAR and GPS ground velocities. Specific results are listed in Table 3 (see supplementary material) that provides, for each GPS station, the velocity differences between geodetic rates, before and after the SAR-GPS integration procedure. We may assess a consistent reduction of both misfits, and corresponding RMSEs, between GPS and SAR-based mean surface velocities, after their integration.

4.2. South-eastern Sicily

Fig. 6 shows the GPS velocity (in the Eurasian-fixed reference frame) and strain-rate fields for SE Sicily. Here, long-term horizontal velocities have been retrieved from both permanent and survey-mode GPS stations, whereas vertical rates have been estimated only from continuous GPS stations. The area exhibits horizontal displacement rates of about 5–6 mm/yr along a NNW attitude (see Fig. 6a) in agreement with the overall motion of the Sicilian block (Mastrolembo Ventura et al., 2014). The strain-rate field has been evaluated on a regular grid of 0.1°, adopting the method described in Palano (2015). It shows that: (a) the northern portion is characterized by a contraction

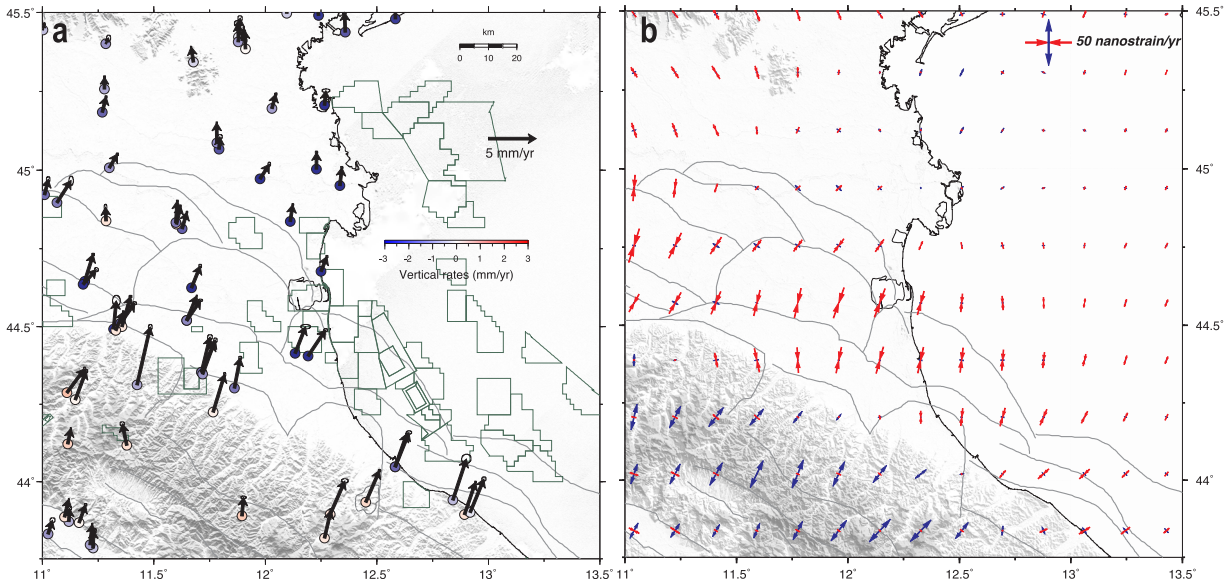

Fig. 4. GPS velocity field over the Ravenna coastal area. (a) Horizontal and vertical velocity field from continuous stations referred to the Eurasian plate. (b) Strain rate field computed over a regular grid, where red and blue arrows refer to compressive and extensional processes, respectively. On-shore and off-shore hydrocarbon reservoirs are shown as green polygons in panel a). (For interpretation of the references to colour in this figure legend, the reader is referred to the web version of this article.)

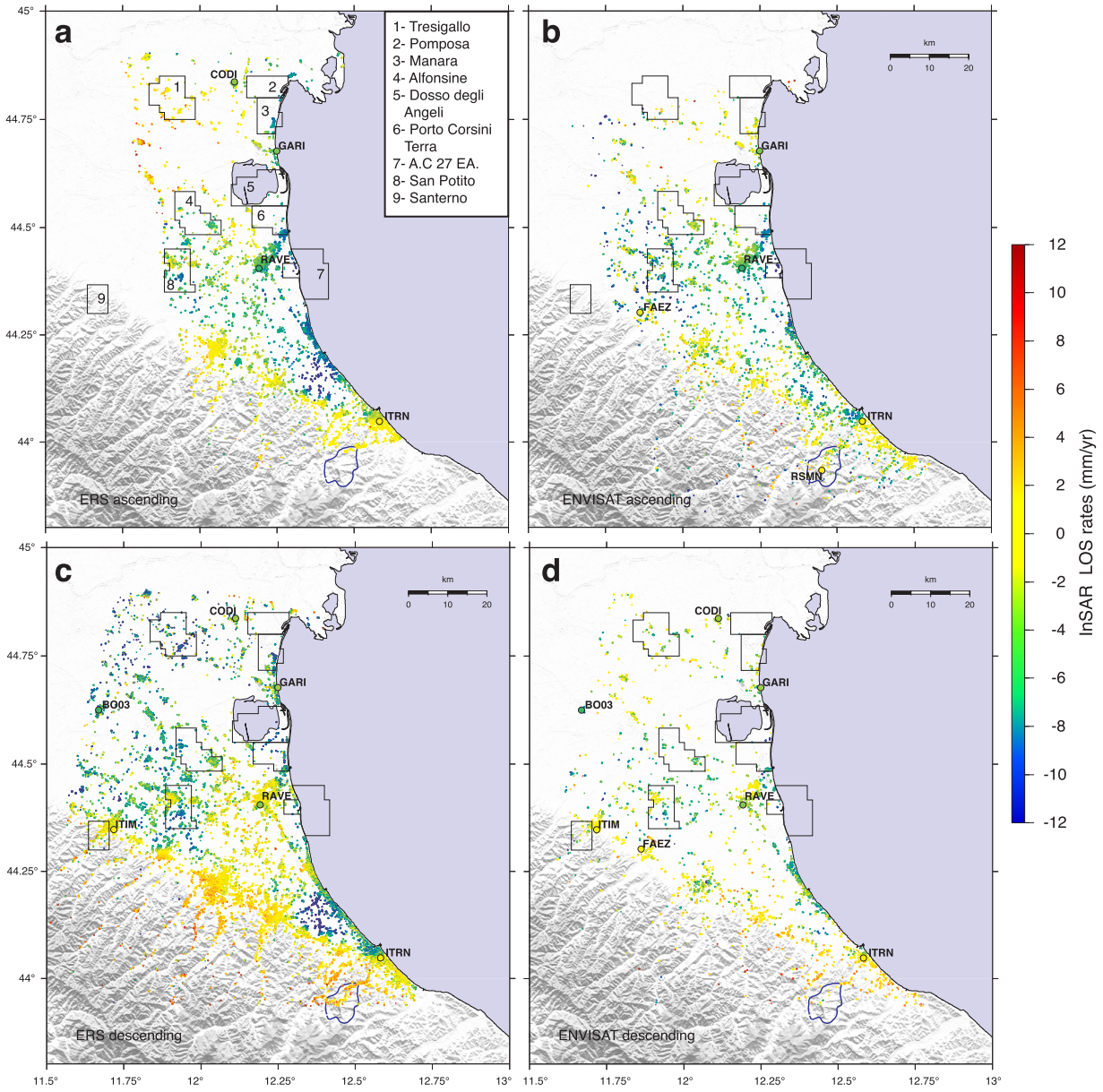

Fig. 5. SAR-based mean surface velocity maps (mm/yr), obtained over Ravenna coastal area with ERS (a, c) and Envisat (b, d) SAR data along ascending (a, b) and descending (c, d) orbits, following the GPS-SAR integration procedure. Colored and labeled circles indicate the 3D GPS velocities projected along the SAR sensor LOS used for each orbit during the datasets integration (Section 3.3).

process, with deformation rates between 100–150 nanostrain/yr and 50–90 nanostrain/yr in the western and eastern portion, respectively; (b) the central part is subjected to extension, with deformation rates between 50–120 nanostrain/yr; (c) the southern portion is characterized by deformation rates below 10 nanostrain/yr (Fig. 6b). Finally, we observe a general positive vertical velocity of 1–2 mm/yr along the coast and the inland areas (Fig. 6a).

Fig. 7 shows the SAR-based LOS mean surface velocity maps of SE Sicily, obtained through ERS and Envisat datasets along ascending and descending orbits, following the GPS-SAR integration procedure. We observe mean negative LOS velocities of about 5 mm/yr, with the highest subsidence rates up to 12 mm/yr along the coastline, in the period 1992–2000 (see ERS-1/2 results in Fig. 7a–c, respectively). Referring to the locations of hydrocarbon reservoirs, we observe positive LOS velocities (i.e., points approaching to the satellite) as sparsely distributed patches along the coastline, especially in the ERS descending dataset (see Fig. 7c). However, such velocities are lower than 1.5 mm/yr, i.e., below the threshold error (+/−2 mm/yr) that is commonly adopted for ERS and Envisat data. Results obtained for the Envisat datasets in the time period 2003–2010 (see Fig. 7b–d) are quite different from those obtained for ERS datasets; in particular, we observe slower subsidence rates with values less than 8 mm/yr.

To assess the consistency of both geodetic results, we have compared multi-temporal DInSAR and GPS velocity fields following the procedure described in Section 3.3. Due to the quite scattered SAR-based velocity maps and the large distances between GPS stations and SAR-pixels, the comparison has been carried out only for the Envisat ascending (Fig. 7b) and ERS descending (Fig. 7c) datasets. In the first case, we have performed the planar correction thanks to the high density of SAR pixels and the good coverage of GPS stations (RMSE = 0.8 mm/yr). In the second case, we have been able to achieve only a first-order comparison between SAR-based and few GPS velocities, showing a relatively good agreement between the two datasets (RMSE = 1.4 mm/yr). Specific results are listed in Table 4 (see supplementary material) that provides, for each GPS station, the differences between the rates obtained using the two geodetic techniques,

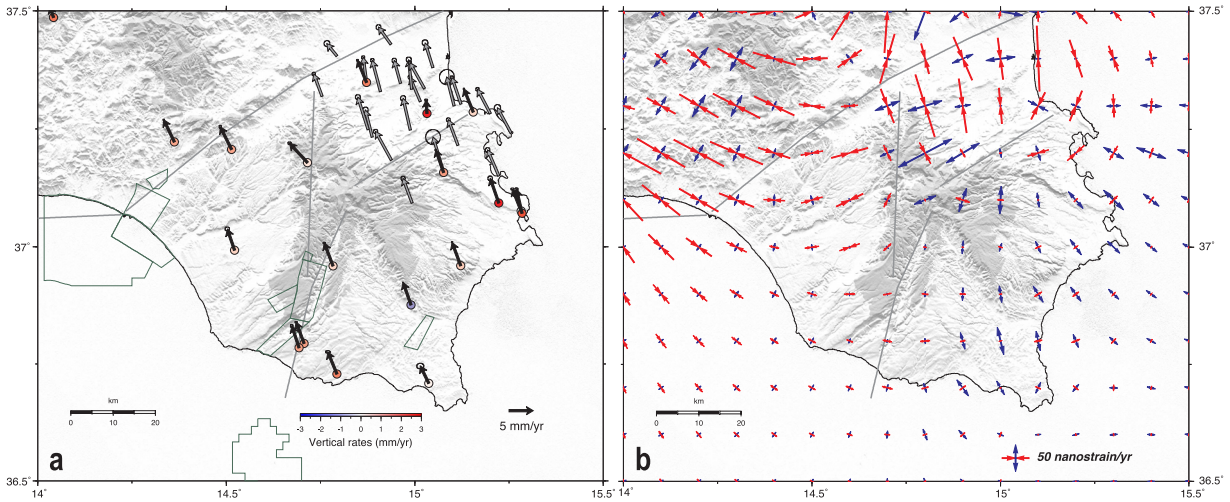

Fig. 6. GPS velocity field over SE Sicily referred to the Eurasian plate. (a) Horizontal velocities from permanent (black) and survey-mode (gray) GPS stations, and vertical displacement rates only from continuous GPS stations. (b) Strain rate field, where red and blue arrows refer to compressive and extensional processes, respectively. (For interpretation of the references to colour in this figure legend, the reader is referred to the web version of this article.)

before and (where possible) after the SAR-GPS integration procedure. Again, we may assess the consistency of both SAR and GPS retrievals for the observed area.

5. Discussion

In this section, we provide a first interpretation of the geodetic results to analyze and assess ground deformation processes. We have compared time series of ground displacements with available

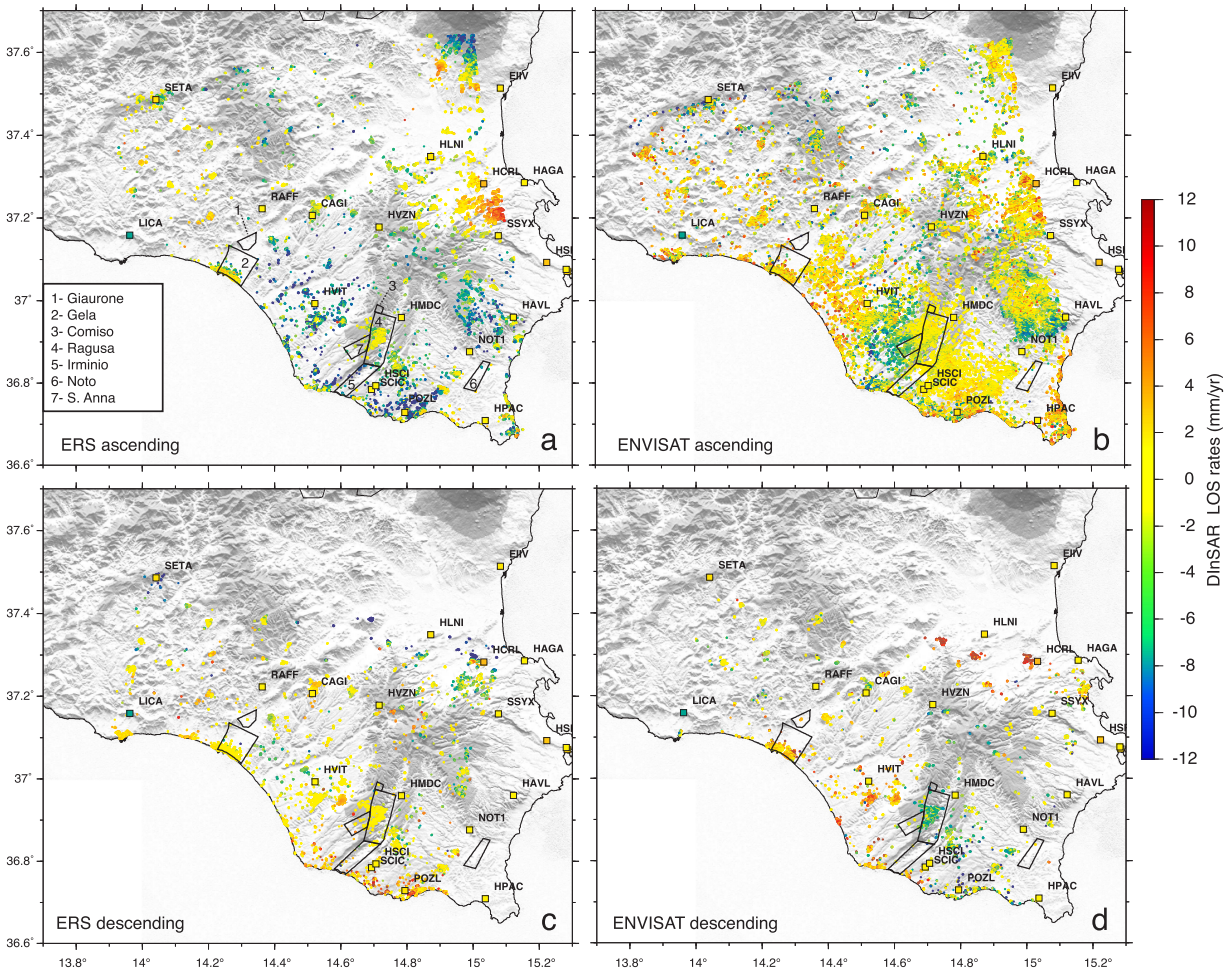

Fig. 7. SAR-based mean surface velocity maps (in mm/yr) obtained over SE Sicily with ERS (a, c) and Envisat (b, d) SAR data along ascending (a, b) and descending (c, d) orbits. 3D GPS velocities projected over SAR sensor LOS (colored and labeled squares) are superimposed to the SAR maps.

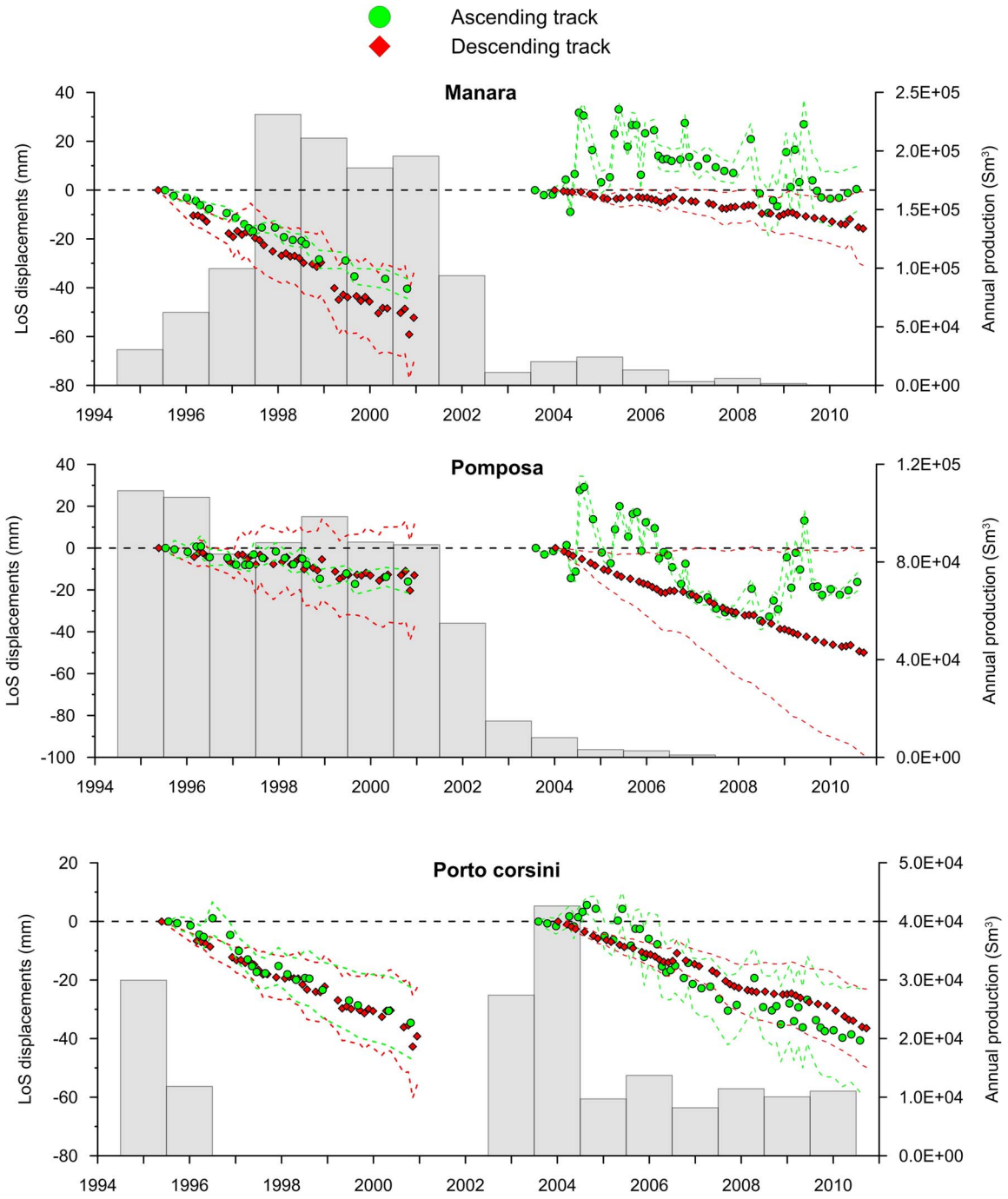

Fig. 8. Comparison between multi-temporal DInSAR time series of LOS surface displacements and hydrocarbon production data (measured as Standard cubic meter − Sm^3) for sample on-shore reservoirs of Ravenna coastal area: (upper panel) Manara, (middle panel) Pomposa and (lower panel) Porto Corsini reservoirs. The mean and the standard deviation values of SAR-based deformations falling within each reservoir, are plotted as big symbols and dotted lines, respectively.

hydrocarbon production data, in order to detect possible spatial and temporal correlation with respect to the on-shore exploitation activities. This comparative analysis allows evaluating the benefits of geodetic protocols for the monitoring of subsidence phenomena along on-shore hydrocarbon reservoirs. In this framework, available GPS stations are far from hydrocarbon reservoirs and the inter-distances among stations are larger than values established by geodetic protocols, i.e., to be less than 10–15 km (Ministero dello Sviluppo Economico, DGS-UNMIG, 2014). Moreover, most of the available GPS stations are located outside the spatial extent of on-shore hydrocarbon reservoirs. As a result, we have not been able to compare GPS products with oil/gas exploitation data. We only performed the comparative analysis between multi-temporal DInSAR products and hydrocarbon reservoirs, which were interested by production activities during the time span of SAR acquisitions.

Data related to the anthropogenic processes are obtained by geological surveys and hydrocarbon production data, freely available at http://unmig.sviluppoeconomico.gov.it/, where yearly production data of each reservoir are provided.

5.1. Ravenna coastal area

GPS horizontal velocities across the whole Ravenna coastal area agree with previous studies (e.g., D'Agostino et al., 2008; Devoti et al.,

2008), highlighting the ongoing convergence between the Apennines and the Adriatic microplate, within the complex Nubia-Eurasia plate boundary zone (see Fig. 4a) (e.g., Malinverno and Ryan, 1986; Faccenna et al., 2003). In agreement with previous results (Montone and Mariucci, 2016; Serpelloni et al., 2005), the strain rate map of the area reveals that the convergence process takes place along the major fold-and-thrust structures of the Ferrara-Romagna arc (Figs. Figure 1a and Figure 4b), where many active hydrocarbon production sites are located (Fig. 2a). In addition, GPS measurements show two subsidence patterns with mean rates of 1–2 mm/yr along the Po Plain and greater than 3 mm/yr along the coasts (Fig. 4a), respectively. The former is mainly related to geologic and tectonic processes (Teatini et al., 2006); whereas the latter and faster ones can be ascribed to anthropogenic phenomena, e.g., groundwater pumping and hydrocarbon exploitation (Kolker et al., 2011; Teatini et al., 2006).

Looking at the SAR-based velocity maps, we observe slow subsidence rates along the coastal area, for both ERS (1992–2000) and Envisat (2003–2010) time-periods (compare Fig. 5a–c with Fig. 5b–d). This contribution accounts for tectonic and geologic processes, as the natural compaction of subsoil (Carbognin et al., 1978, 1984; Galloway et al., 1999; Galloway and Hoffmann, 2007; Gambolati et al., 1999; Svigkas et al., 2016, 2017; Teatini et al., 2005, 2006; Zhou et al., 2009). Comparing ERS and Envisat results, we may assess that ground deformation patterns have shown similar trends in the whole time period 1992–2010. In detail, Ravenna and SE coastlines show an intense subsidence, with velocities greater than 5 mm/yr (see blue and green patches in Fig. 5). These faster rates may be related both to the groundwater pumping from shallow aquifers and deep hydrocarbon reservoir exploitation (Gambolati et al., 1991; Pieri and Groppi, 1981; Teatini et al., 2005, 2006).

Multi-temporal DInSAR results agree with both GPS velocities and previous geodetic investigations in the pilot area, obtained by the Regional Agency for the Prevention, the Environment and the Energy of Emilia Romagna region (ARPAE) (Bitelli et al., 2012; Ministero dello Sviluppo Economico, 2013; Regione Emilia-Romagna-Arpa Emilia-Romagna, 2012). In detail, we confirm the displacement trends, previously observed in some areas of the test site. For example, the provinces located in the NW inland and along the Eastern coastline exhibit constant subsidence rates, with velocities of about 2–4 mm/yr. Other provinces located along the northern coast and the SE inland area exhibit an increasing subsidence, with mean rates of 4–5 mm/yr. Moreover, we observe faster subsidence rates of about 6–7 mm/yr along the coast. All these phenomena can be likely related to the groundwater pumping for industrial, civil and irrigation purposes.

In the following, we compare multi-temporal DInSAR results to hydrocarbon exploitation activities. In detail, Fig. 8 shows geodetic results as colored plots against production data, which are imaged as background gray histograms. For comparison purposes, we have evaluated the mean and the standard deviation values of multi-temporal DInSAR displacements within each reservoir (see the big symbols and dotted lines in Fig. 8, respectively).

We observe that SAR-based displacement time series exhibit a non-linear behavior and large scattered variability along ascending orbits (see the green circles in Fig. 8). This is evident especially when considering the Envisat results, thus making the interpretation of DInSAR results very challenging. Conversely, we observe less scattered displacement time series for SAR datasets acquired along the descending orbit (see red diamonds in Fig. 8). In detail, ERS and Envisat SAR time series show linear negative trends (i.e., subsidence) over all the selected reservoirs. Looking at the standard deviation values of SAR-based displacements (see the dotted-line plots in Fig. 8), we observe a large variability for both ERS and Envisat time series, especially along the descending orbit (red-colored plots). This result highlights a non-uniform deformation pattern along the spatial extent of each reservoir. It reveals that local heterogeneous factors (i.e., natural processes and/or anthropogenic activities) strongly affect multi-temporal DInSAR displacements. Based on the temporal and spatial variability of SAR-based results, we suppose that the observed displacements are ascribed to the groundwater exploitation from shallow aquifers. This assumption takes into account the subsoil properties and the nature of deformation phenomena related to groundwater pumping activities (i.e., slow, irreversible and time-continuous subsidence, see Modoni et al., 2013; Teatini et al., 2006). Indeed, these processes are spatially localized with linear trends over the entire observational time-span and may be correlated to near-surface strata of subsoil, where groundwater aquifers are located.

Looking at the Envisat SAR time series, subsidence rates exhibit slower mean velocities than those obtained from ERS SAR datasets, thus suggesting a progressive reduction of subsidence rates (see the case studies of Manara and Porto Corsini reservoirs in Fig. 8). Conversely, the Pomposa reservoir shows an increase of subsidence rates when comparing Envisat and ERS time series. These results agree with historic surveys of the pilot areas (Bitelli et al., 2012; Ministero dello Sviluppo Economico, 2013; Regione Emilia-Romagna-Arpa Emilia-Romagna, 2012), which correlated the SAR-based displacement time series to groundwater exploitation activities from shallow aquifers.

In agreement with current and previous literature studies (Modoni et al., 2013; Teatini et al., 2006), we observe that multi-temporal DInSAR time series of surface deformations do not show a clear temporal correlation with hydrocarbon production data, for all the selected on-shore reservoirs. In fact, the increase or the reduction of hydrocarbon extraction activities does not affect the subsidence rates. This is evident observing the results obtained for Pomposa and Porto Corsini reservoirs (see middle and lower panels in Fig. 8, respectively). Moreover, the large spatial variability provided by the standard deviation values of multi-temporal DInSAR time series highlights heterogeneous deformation patterns along each reservoir. Commonly, deep hydrocarbon production activities are responsible for homogenous displacement patterns, along a spatial extent that is comparable to the depth of each reservoir. Hence, based on our experimental results, we may exclude that the oil/gas exploitation has induced the observed multi-temporal DInSAR displacements. However, an interesting case study is Manara (see the upper panel in Fig. 8), where the reduction of subsidence rates in the time span 1992–2010 could be correlated to the reduced exploitation activity of the reservoir.

More in situ information and geodetic measurements are needed to provide a robust analysis of any possible correlation between geodetic measurements and oil/gas exploitation activities. Fig. 9 highlights the limits of the proposed approach:

- The poor availability of spatially dense SAR-based measurements in correspondence of each reservoir, for either acquisition time period or satellite orbit (see the case study of Santerno reservoir in Fig. 9);
- The lack of hydrocarbon production data, due to the dismissing or the reduced exploitation of the reservoir (see Alfonsine and Dosso degli angeli reservoirs, respectively, in Fig. 9).

5.2. South-eastern Sicily

Horizontal GPS velocities highlights that the present-day convergence between the Nubia and Eurasia plates is accommodated at the frontal thrusts of the northern Hyblean margin (see Fig. 6a). Moreover, the Hyblean Plateau is separated in two blocks (the western and the eastern ones) by the left-lateral strike-slip faulting, as previously described (e.g., Mastrolembo Ventura et al., 2014; Musumeci et al., 2014 and references therein). All these features are also emphasized by the strain-rate field (see Fig. 6b), which reveals a complex heterogeneous geological and tectonic framework. In addition, we observe slow subsidence rates (see Fig. 6a), which are mainly due to the complex interplay of subsidence and uplift processes, associated with regional tectonics and local-scale anthropogenic contributions, e.g., large-volume groundwater pumping for agricultural, industrial and potable

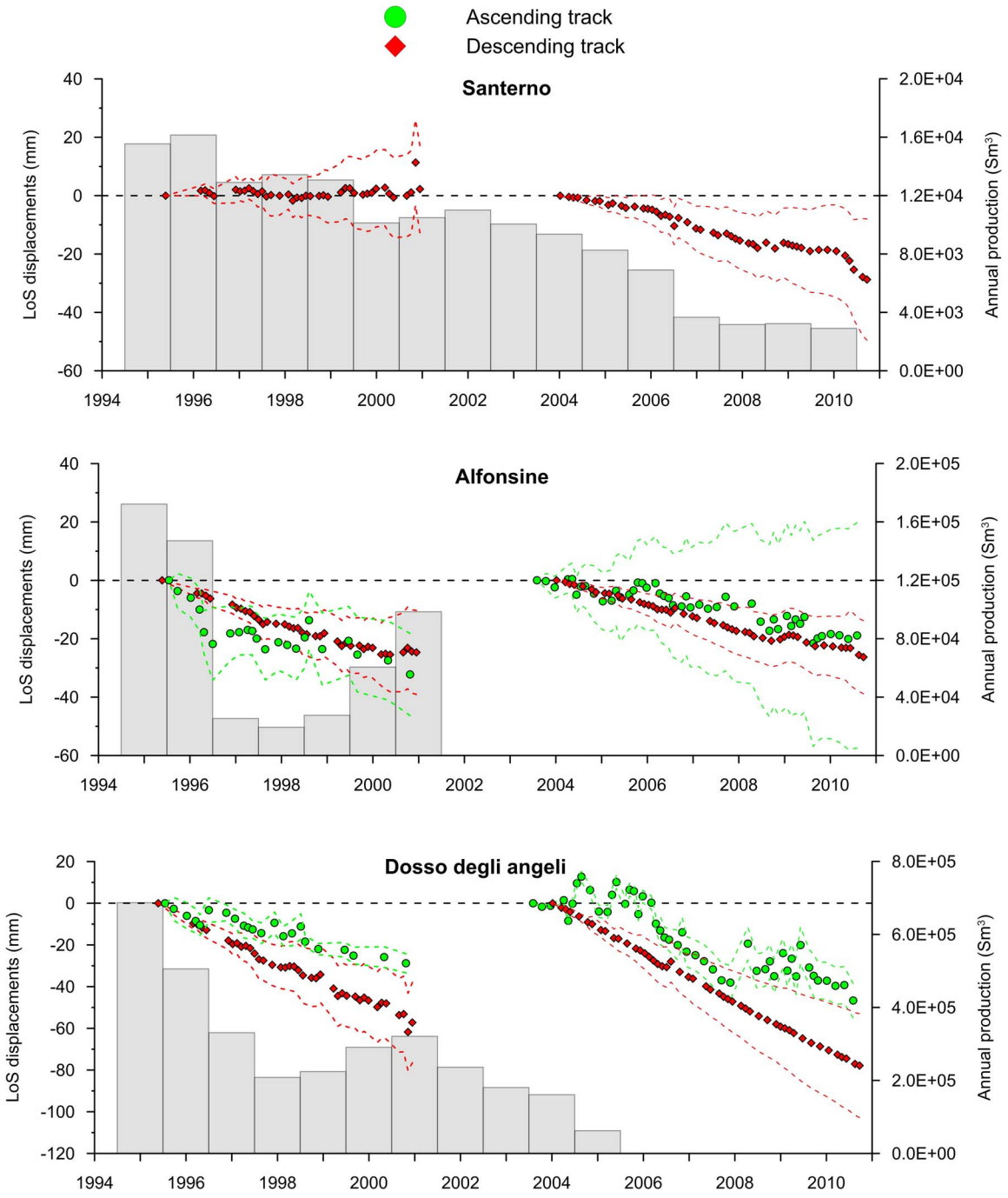

Fig. 9. Comparison between multi-temporal DInSAR time series of LOS surface displacements and hydrocarbon production data (measured as Standard cubic meter – Sm^3) for sample on-shore reservoirs of Ravenna coastal area, characterized by either lack or reduced amount of data: (upper panel) Santerno, (middle panel) Alfonsine and (lower panel) Dosso degli angeli reservoirs.

purposes (Aureli et al., 1987; Serpelloni et al., 2013; Vollrath et al., 2017).

Looking at the multi-temporal DInSAR products, ERS-1/2 results (see Fig. 7a–c) highlight non-negligible subsidence processes along the coastline in the time period 1992–2000. However, we observe high subsidence rates for some urban areas located in the southernmost sector of the pilot area, together with localized uplift phenomena in SW coastal villages. The Envisat velocity maps for the time period 2003–2010 (see Fig. 7b–d) slightly agree with those obtained with ERS datasets: indeed, slower and faster subsidence rates may be observed along ascending and descending orbit, respectively.

Patterns of multi-temporal DInSAR velocities, obtained from ERS and Envisat data (Fig. 7a–c and Fig. 7b–d), are in agreement with previous geodetic studies of the area (e.g., Serpelloni et al., 2013; Vollrath et al., 2017). We observe no significant changes in the subsidence trend during the SAR observational time spans, with mean rates between 1–5 mm/yr (see the southern inland area). SW and SE coasts exhibit a decreasing subsidence, with mean rates of about 2–5 mm/yr. Moreover, we identify localized areas with increasing subsidence rates along the southern coastline, with maximum velocities of about 7 mm/yr.

Furthermore, we have compared multi-temporal DInSAR displacement time series to hydrocarbon production data for sample on-shore reservoirs (see Fig. 10). Experimental results show that mean surface

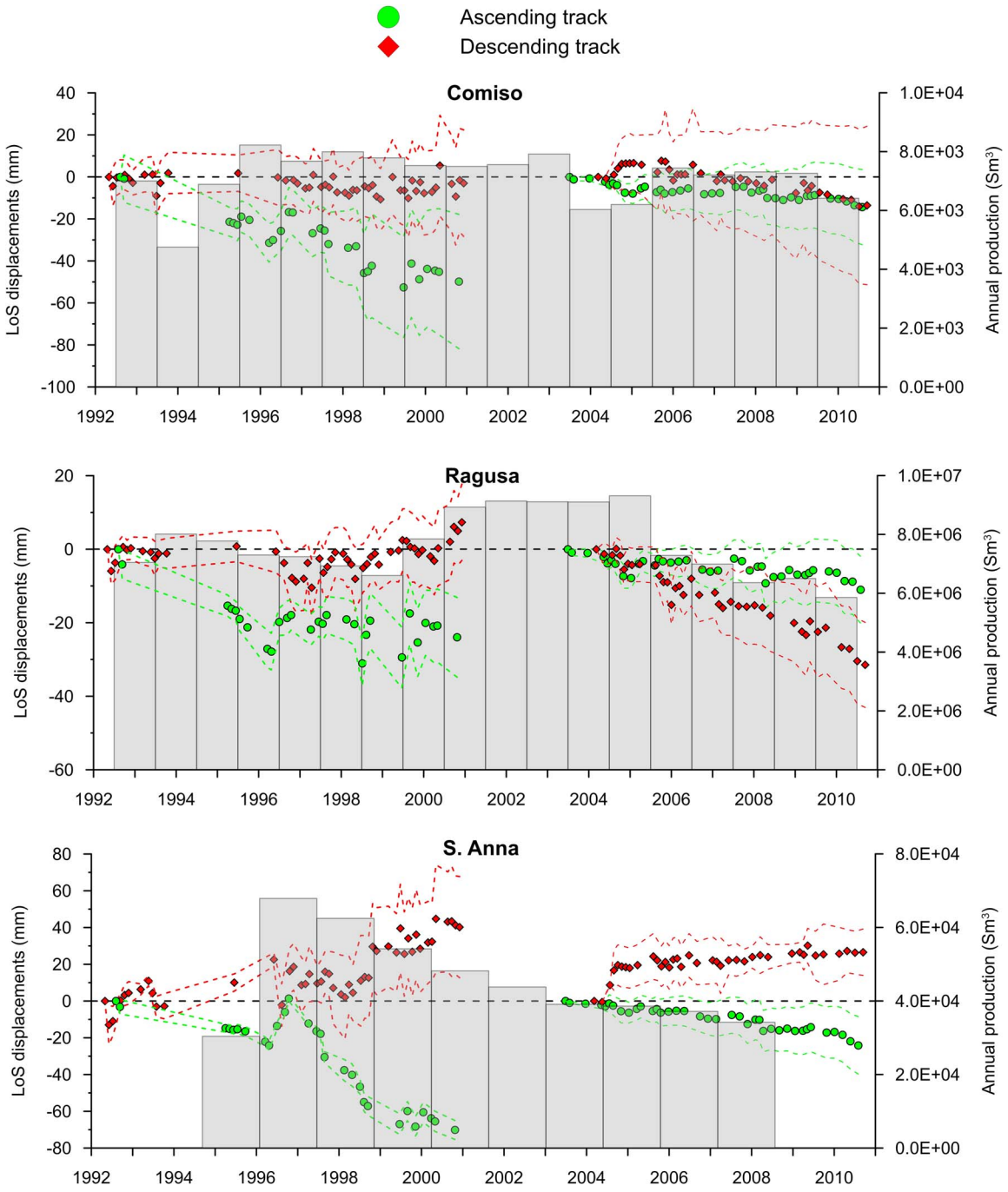

Fig. 10. Comparison between multi-temporal DInSAR time series of LOS surface displacements and hydrocarbon production data (measured as Standard cubic meter − Sm^3) for sample on-shore reservoirs of SE Sicily. (upper panel) Comiso, (middle panel) Ragusa, (lower panel) S. Anna hydrocarbon reservoirs.

deformations (see big symbols plots) retrieved with ERS datasets exhibit a large random variability with respect to those obtained with Envisat data, along both ascending and descending orbits. Moreover, we observe large standard deviations of SAR-based displacement time series along both acquisition orbits (see dotted-line plots in Fig. 10). Both results highlight the presence of heterogeneous deformation patterns in both time and space, thus making the interpretation of results very challenging. Again, we observe a non-negligible dependency of multi-temporal DInSAR results with respect to localized ground deformation processes (see sparsely distributed plots in Fig. 10).

Comparing ERS and Envisat SAR time series, subsidence measurements show linear trends in the whole time period 1992–2010. In detail, Envisat results reveal stable and slower subsidence rates than those observed with ERS datasets, thus enhancing a stability and reduction of subsidence processes over the time, respectively. Considering the heterogeneous deformation pattern retrieved by multi-temporal DInSAR in terms of mean and standard deviation values, we suppose that the observed deformation can be related to groundwater exploitation from shallow aquifers. Indeed, this latter activity is responsible for slow, irreversible and time-continuous subsidence, with linear temporal trend and non-uniform distribution (Albano et al., 2016; Chaussard et al., 2014; Stramondo et al., 2007).

Finally, we observe that multi-temporal DInSAR results are not correlated with oil/gas production data for all the selected reservoirs. Indeed, the increase or reduction of hydrocarbon extraction does not affect the subsidence rates retrieved through SAR data, which further

provide rather heterogeneous subsidence patterns. Conversely, hydrocarbon production is expected to be responsible for uniform homogeneous deformations, along a spatial extent comparable to the depth of reservoirs (Allison et al., 2014; Kolker et al., 2011). We need more geodetic networks with dense and time-continuous measurements of ground displacements, to analyze the impact of hydrocarbon exploitation over land subsidence processes and geodetic observations.

6. Conclusions and outlooks

In this study, we applied protocols based on the "Addresses and Guidelines" established by MISE, for monitoring subsidence phenomena potentially related to Oil and Gas exploitation activities from on-shore reservoirs. Such protocols are based on the analysis of multi-temporal GPS and DInSAR displacement time series. Here we focused on the Ravenna coastline and SE Sicily. For the two pilot areas, we integrated GPS measurements, collected during the 1995–2016 time interval, with multi-temporal DInSAR products retrieved through the SBAS processing of ERS and Envisat acquisitions covering the 1992–2010 timespan.

As already demonstrated, GPS allowed to precisely describe crustal deformation processes related to ongoing tectonic and geologic processes at regional scale. However, the current density and geographical distribution of the available GPS networks cannot provide the sufficient spatial resolution, able to catch the potential localized displacements related to the hydrocarbon production. The proposed methodology requires dense GPS networks on the top and around the exploitation areas. On the other hand, multi-temporal DInSAR displacement rates, calibrated by GPS velocities at larger scale, allowed observing subsidence patterns related to natural and anthropogenic processes, with a revisit-time of monthly sample rate, a ground coverage of about tens of km^2 and an accuracy of few millimeters. In this case, the spatial resolution (about tens of meters) is high and reasonably sufficient for monitoring large reservoirs. However, the time resolution of ERS and Envisat data is low (weeks to months) and the comparison with hydrocarbon production data is possible only in terms of overall long-term trends and not for rapid transient deformations.

The comparison between multi-temporal DInSAR displacement time series and hydrocarbon production data showed a poor correlation between geodetic trends and deep hydrocarbon exploitation data. However, some limits must be taken into account, e.g., the presence of dismissed reservoirs, the poor spatial/temporal availability of production data, the different sample rate of SAR retrievals and hydrocarbon exploitation data.

The proposed geodetic protocols show some critical issues, e.g., the high complexity of processing techniques, the non-negligible spatial and temporal decorrelations of multi-temporal DInSAR datasets, the lack of dense and time-extended GPS data within on-shore reservoirs, the poor availability of in situ ground truth about groundwater pumping and hydrocarbon exploitation activities. On this basis, we may list some improvements of MISE guidelines for the effective geodetic monitoring of hydrocarbon reservoirs:

- Long-time-extended SAR data along ascending and descending orbits, with monthly sampling rate and few-meter resolution. In this framework, the availability of current and future operational SAR constellation missions (e.g., COSMO-SkyMed, TerraSAR, Sentinel-1, RADARSAT, ALOS-PALSAR) can provide several benefits to improve monitoring capabilities, in terms of multi-frequency acquisitions (X-, C-, L-bands), multi-resolution images (up to 1.5 m for TerraSAR), multi-spatial coverage (from 40 km^2 for COSMO-SkyMed up to 200 km^2 for Sentinel-1), reduced revisit-time (availability of multiple satellites for each constellation), large numbers of available InSAR pairs (it allows improving the retrieval and the removal of topographic phase residuals because of multiple perpendicular baselines);
- The integration of the proposed multi-temporal DInSAR technique with Persistent Scatterer Interferometry (PSI) approaches (Crosetto et al., 2016), such as SqueeSAR algorithm (Ferretti et al., 2001, 2011). These methods can be considered complementary to the SBAS approach, providing punctual deformation, at subpixel scale (single scatterer) and with high density, giving additional data to help monitoring local-scale heterogeneous subsidence processes;
- High-resolution DEM (e.g., SRTM-30m, TINITALY-10m, TanDEM-X-12m, SPOT6-8m, Pléiades-1m). Some properties should be considered in DEM selection for multi-temporal DInSAR topography phase removal, such as: the DEM vertical accuracy (a theoretical limit of $\lambda/4$ should be ensured as maximum DEM inaccuracy, i.e., 0.75 cm, 1.37 cm and 6 cm for X-, C- and L-band, respectively); the DEM spatial resolution (i.e., its capability to reconstruct horizontal terrain gradients) compared to the ones of DInSAR products; whether DEM is up-to-date with regards to InSAR timeline (Hanssen, 2001);
- The installation of GPS stations within hydrocarbon reservoirs and artificial PS (e.g., corner reflectors) in case of GPS stations located along incoherent areas of SAR displacement maps;
- More timely and spatially co-located in situ data and historical information about hydrocarbon reservoir.

Acknowledgements

Authors thank ESA for providing ERS and Envisat SAR data used in this work. The present work is supported and funded by the Italian Ministry of Economic Development (MISE) under the MISE-DGRME research project (ID 0752.010). We wish to thank Prof. Freek van der Meer for the editorial handling of the manuscript and anonymous reviewers for their useful suggestions.

Appendix A. Supplementary data

Supplementary data associated with this article can be found, in the online version, at https://doi.org/10.1016/j.jag.2018.02.011.

References

Albano, M., Polcari, M., Bignami, C., Moro, M., Saroli, M., Stramondo, S., 2016. An innovative procedure for monitoring the change in soil seismic response by InSAR data: application to the Mexico City subsidence. Int. J. Appl. Earth Obs. Geoinf. 53, 146–158. http://dx.doi.org/10.1016/j.jag.2016.08.011.

Allison, M., Yuill, B., Törnqvist, T., Amelung, F., Dixon, T., Erkens, G., Stuurman, R., Jones, C., Milne, G., Steckler, M., Syvitski, J., Teatini, P., 2014. Global risks and research priorities for coastal subsidence. EOS 97, 22–27. http://dx.doi.org/10.1029/2016EO055013.

Amato, A., Azzara, R., Basili, A., Chiarabba, C., Cocco, M., Di Bona, M., Selvaggi, G., 1995. Main shock and aftershocks of the December 13, 1990, eastern Sicily earthquake. Ann. Geofis. 38, 255–266. http://dx.doi.org/10.4401/ag-4122.

Amelung, F., Galloway, D.L., Bell, J.W., Zbeker, H.A., Laczniak, R.J., 1999. Sensing the ups and downs of Las Vegas: inSAR reveals structural control of land subsidence and aquifer-system deformation. Geology 27 (6), 483–486. http://dx.doi.org/10.1130/0091-7613(1999)027<0483:STUADO>2.3.CO;2.

Anderlini, L., Serpelloni, E., Belardinelli, M.E., 2016. Creep and locking of a low-angle normal fault: insights from the Altotiberina fault in the Northern Apennines (Italy). Geophys. Res. Lett. 43 (9), 4321–4329. http://dx.doi.org/10.1002/2016GL068604.

Antonioli, F., Anzidei, M., Amorosi, A., Lo Presti, V., Mastronuzzi, G., Deiana, G., De Falco, G., Fontana, A., Fontolan, G., Lisco, S., Marsico, A., Moretti, M., Orrù, P.E., Sannino, G.M., Serpelloni, E., Vecchio, A., 2017. Sea-level rise and potential drowning of the Italian coastal plains: flooding risk scenarios for 2100. Quat. Sci. Rev. 158, 29–43. http://dx.doi.org/10.1016/j.quascirev.2016.12.021.

Aureli, A., Adorni, G., Chiavetta, A.F., Fazio, F., 1987. Condizioni di vulnerabilità di acquiferi in zone a forte insediamento industriale di tipo petrolchimico. Mem. Soc. Geol. Ital. 37, 35–52.

Bamler, R., Hartl, P., 1998. Synthetic aperture radar interferometry. Inverse Prob. 14, 1–54. http://dx.doi.org/10.1088/0266-5611/14/4/001.

Bell, J.W., Amelung, F.A., Ferretti, A., Bianchi, M., Novali, F., 2008. Permanent scatterer InSAR reveals seasonal and long-term aquifer-system response to groundwater pumping and artificial recharge. Water Resour. Res. 44 (2), 2407–2425. http://dx.doi.org/10.1029/2007WR006152.

Bennett, R.A., Serpelloni, E., Hreinsdóttir, S., Brandon, M.T., Buble, G., Basic, T., Casale, G., Cavaliere, A., Anzidei, M., Marjonovic, M., Minelli, G., Molli, G., Montanari, A., 2012. Syn-convergent extension observed using the RETREAT GPS network, northern

Apennines, Italy. J. Geophys. Res. 117, B04408. http://dx.doi.org/10.1029/2011JB008744.
Berardino, P., Fornaro, G., Lanari, R., Sansosti, E., 2002. A new algorithm for surface deformation monitoring based on small baseline differential SAR interferograms. IEEE Trans. Geosci. Remote Sens. 40, 2375–2383. http://dx.doi.org/10.1109/TGRS.2002.803792.
Bertello, F., Fantoni, R., Franciosi, R., Gatti, V., Ghielmi, M., Pugliese, A., 2010. From thrust-and-fold belt to foreland: hydrocarbon occurrences in Italy. In Geological Society, London, Petroleum Geology Conference Series 7, 113–126. http://dx.doi.org/10.1144/0070113.
Beutler, G., Moore, A.W., Mueller, I.I., 2008. The international global navigation satellite systems (GNSS) service: developments and achievements. J. Geodesy 83 (3–4), 297–307. http://dx.doi.org/10.1007/s00190-008-0268-z.
Billi, A., Porreca, M., Faccenna, C., Mattei, M., 2006. agnetic and structural constraints for the noncylindrical evolution of a continental forebulge (Hyblea, Italy). Tectonics 25http://dx.doi.org/10.1029/2005TC001800. (TC3011).
Bitelli, G., Bonsignore, F., Del Conte, S., Pellegrino, I., Vittuari, L., 2012. Subsidence monitoring at regional scale in Emilia-Romagna. In: Proc. of 7th European Congress on Regional Geoscientific Cartography and Information Systems (EUREGEO). Bologna, June 12–15. pp. 740–741.
Bonì, R., Meisina, C., Perotti, C., Fenaroli, F., 2015. PSI-based methodology to land subsidence mechanism recognition. Proc. of International Association of Hydrological Sciences (IAHS) 372, 357–360. http://dx.doi.org/10.5194/piahs-372-357-2015.
Boschi, E., Guidoboni, E., Ferrari, G., Mariotti, D., Valensise, G., Gasperini, P., 2000. Catalogue of strong italian earthquakes from 461 B. C. to. Ann. Geof. 43, 609–868. http://dx.doi.org/10.4401/ag-3668.
Cannavò, F., Palano, M., 2015. Defining geodetic reference frame using matlab: platEMotion 2.0. Pure Appl. Geophys. 173 (3), 937–944. http://dx.doi.org/10.1007/s00024-015-1112-z.
Carbognin, L., Gatto, P., Mozzi, G., Gambolati, G., 1978. Land subsidence of Ravenna and its similarities with the Venice case. In: Saxena, S.K. (Ed.), Evaluation and Prediction of Subsidence, pp. 254–266 (Am. Soc. of Civ. Eng., Reston,V a.).
Carbognin, L., Gatto, P., Mozzi, G.G., 1984. Case history no.9.15: Ravenna, Italy. In: Poland, J.F. (Ed.), Guidebook to Studies of Land Subsidence Due to Ground-Water Withdrawal, pp. 291–305 (U.N. Educ. Sci. and Cultural Organ., Paris).
Casero, P., Bigi, S., 2013. Structural setting of the Adriatic basin and the main related petroleum exploration plays. Mar. Petrol. Geol. 42, 135–147. http://dx.doi.org/10.1016/j.marpetgeo.2012.07.006.
Casero, P., 2004. Structural Setting of Petroleum Exploration Plays in Italy. Special Volume of the Italian Geological Society for the IGC 32 Florence-2004. pp. 189–199.
Catalano, S., De Guidi, G., Romagnoli, G., Torrisi, S., Tortorici, G., Tortorici, L., 2008. The migration of plate bound-aries in SE Sicily: influence on the large-scale kinematic model of the African promontory in southern Italy. Tectonophysics 449 (1–4), 41–62. http://dx.doi.org/10.1016/j.tecto.2007.12.003.
Catalano, S., Romagnoli, G., Tortorici, G., 2010. Kinematics and dynamics of the late Quaternary rift-flank deformation in the Hyblean Plateau (SE Sicily). Tectonophysics 486, 1–14. http://dx.doi.org/10.1016/j.tecto.2010.01.013.
Chahoud, A., Zavatti, A., 1999. Stato ambientale (quali-quantitativo) delle acque sotterranee: L'acquifero Emiliano Romagnolo. Quaderni Geol. Appl. 2 (Suppl. 1999) (3.365).
Chaussard, E., Wdowinski, S., Cabral-Cano, E., Amelung, F., 2014. Land subsidence in central Mexico detected by ALOS InSAR time-series. Remote Sens. Environ. 140 (0), 94–106. http://dx.doi.org/10.1016/j.rse.2013.08.038.
Crosetto, M., Monserrat, O., Cuevas-González, M., Devanthéry, N., Crippa, B., 2016. Persistent scatterer interferometry: a review. ISPRS J. Photogramm. Remote Sens. 115, 78–89. http://dx.doi.org/10.1016/j.isprsjprs.2015.10.011.
D'Agostino, N., Avallone, A., Cheloni, D., D'Anastasio, E., Mantenuto, S., Selvaggi, G., 2008. Active tectonics of the Adriatic region from GPS and earthquake slip vectors. J. Geophys. Res. 113, B12413. http://dx.doi.org/10.1029/2008JB005860.
DISS Working Group, 2015. Database of Individual Seismogenic Sources (DISS), Version 3.2.0: A Compilation of Potential Sources for Earthquakes Larger than M 5.5 in Italy and Sur-Rounding Areas. http://dx.doi.org/10.6092/INGV.IT-DISS3.2.0.. http://diss.rm.ingv.it/diss, © INGV 2015 ? Istituto Nazionale di Geofisica e Vulcanologia.
Devoti, R., Riguzzi, F., Cuffaro, M., Doglioni, C., 2008. New GPS constraints on the kinematics of the Apennines subduction. Earth Planet. Sci. Lett. 273 (1-2), 163–174. http://dx.doi.org/10.1016/j.epsl.2008.06.031.
Devoti, R., Esposito, A., Pietrantonio, G., Pisani, A.R., Riguzzi, F., 2011. Evidence of large scale deformation patterns from GPS data in the Italian subduction boundary. Earth Planet. Sci. Lett. 311 (3–4), 230–241. http://dx.doi.org/10.1016/j.epsl.2011.09.034.
Doglioni, C., 1993. Some remarks on the origin of foredeeps. Tectonophysics 228 (1–2), 1–20. http://dx.doi.org/10.1016/0040-1951(93)90211-2.
Dokka, R.K., 2006. Modern-day tectonic subsidence in coastal Louisiana. Geology 34, 281–284. http://dx.doi.org/10.1130/G22264.1.
Dow, J.M., Neilan, R.E., Rizos, C., 2009. The international GNSS service in a changing landscape of global navigation satellite systems. J. Geod. 83 (3–4), 191–198. http://dx.doi.org/10.1007/s00190-008-0300-3.
Faccenna, C., Becker, T.W., Lucente, F.P., Jolivet, L., Rossetti, F., 2001. History of subduction and back arc extension in the Central Mediterranean. Geophys. J. Int. 145 (3), 809–820. http://dx.doi.org/10.1046/j.0956-540x.2001.01435.x.
Faccenna, C., Jolivet, L., Piromallo, C., Morelli, A., 2003. Subduction and the depth of convection in the Mediterranean mantle. J. Geophys. Res. 108 (B2), 2099. http://dx.doi.org/10.1029/2001JB00169.
Faccenna, C., Becker, T.W., Miller, M.S., Serpelloni, E., Willett, S.D., 2014. Isostasy, dynamic topography, and the elevation of the Apennines of Italy. Earth Planet. Sci. Lett. 407 (C), 163–174. http://dx.doi.org/10.1016/j.epsl.2014.09.027.
Ferretti, A., Prati, C., Rocca, F., 2001. Permanent scatterers in SAR interferometry. IEEE Trans. Geosci. Remote Sens. 39 (1), 8–20. http://dx.doi.org/10.1109/36.898661.
Ferretti, A., Fumagalli, A., Novali, F., Prati, C., Rocca, F., Rucci, A., 2011. A new algorithm for processing interferometric data-stacks: squeeSAR. IEEE Trans. Geosci. Remote Sens. 49 (9), 3460–3470. http://dx.doi.org/10.1109/TGRS.2011.2124465.
Galloway, D.L., Hoffmann, J., 2007. The application of satellite differential SAR interferometry-derived ground displacements in hydrogeology. Hydrogeol. J. 15, 133–154. http://dx.doi.org/10.1007/s10040-006-0121-5.
Galloway, D.L., Jones, D.R., Ingebritsen, S.E., 1999. Land Subsidence in the United States. U.S. Geological Survey Circular, pp. 1182.
Gambolati, G., Ricceri, G., Bertoni, W., Brighenti, G., Vuillermin, E., 1991. Mathematical simulation of the subsidence of Ravenna. Water Resour. Res. 27 (11), 2899–2918. http://dx.doi.org/10.1029/91WR01567.
Gambolati, G., Teatini, P., Tomasi, L., Gonella, M., 1999. Coastline regression of the Romagna Region, Italy, due to sea level rise and natural and anthropogenic land subsidence. Water Resour. Res. 35 (1), 163–184. http://dx.doi.org/10.1029/1998WR900031.
Ghisetti, F., Vezzani, L., 1980. The structural features of the Iblean plateau and of the Monte Iudica area (South Eastern Sicily). A microtectonic contribution to the deformational history of the Calabrian Arc. Bollettino della Società Geologica Italiana 99, 57–102.
Granath, J.W., Casero, P., 2004. Tectonic setting of the petroleum systems of Sicily. In: In: Swennen, R., Roure, F., Granath, J.W. (Eds.), Deformation, Fluid Flow, and Reservoir Appraisal in Foreland Fold and Thrust Belts, vol 1. AAPG Hedberg Series, pp. 391–411.
Grasso, M., Reuther, C.D., 1988. The western margin of the Hyblean Plateau: a neotectonic transform system on the SE Sicilian foreland. Ann. Tecton. 2, 107–120.
Grasso, M., Behncke, B., Di Geronimo, I., Giuffrida, S., La Manna, F., Maniscalco, R., Pedley, H.M., Raffi, S., Schmincke, H.U., Strano, D., Sturiale, G., 2004. Carta geologica del bordo nord-occidentale dell'Avampaese Ibleo e del fronte della Falda di Gela. (Firenze: S.EL.C.A.).
Guglielmino, F., Bignami, C., Bonforte, A., Briole, P., Obrizzo, F., Puglisi, G., Stramondo, S., Wegmüller, U., 2011. Analysis of satellite and in situ ground deformation data integrated by the SISTEM approach: the April 3, 2010 earthquake along the Pernicana fault (Mt. Etna-Italy) case study. Earth Planet. Sci. Lett. 312 (3–4), 327–336. http://dx.doi.org/10.1016/j.epsl.2011.10.028.
Hanssen, R.F., 2001. Radar Interferometry: Data Interpretation and Error Analysis. Kluwer Academic Publishers, Dordrecht, pp. 328 (ISBN 0–7923-6945-9).
Herring, T., King, R.W., McClusky, S., 2010. GAMIT Reference Manual. Release 10.4. Massachussetts Institute of Technology, Cambridge, MA.
Heywood, C.E., Pope, J.P., 2009. Simulation of Ground-Water Flow in the Coastal Plain Aquifer System of Virginia. U.S. Geological Survey Scientific Investigations Report 2009–5039. pp. 115. available at: http://pubs.usgs.gov/sir/2009/5039 (Accessed November 9, 2017).
INGV RING Working Group, 2016. Rete Integrata Nazionale GPS. http://dx.doi.org/10.13127/RING.
Keranen, K.M., Weingarten, M., Abers, G.A., Bekins, B.A., Ge, S., 2014. Sharp increase in central Oklahoma seismicity since 2008 induced by massive wastewater injection. Science 345 (6195), 448–451. http://dx.doi.org/10.1126/science.1255802.
Kolker, A.S., Allison, M.A., Hameed, S., 2011. An evaluation of subsidence rates and sealevel variability in the northern Gulf of Mexico. Geophys. Res. Lett. 38, L21404. http://dx.doi.org/10.1029/2011GL049458.
Malinverno, A., Ryan, W.B.F., 1986. Extension in the Tyrrhenian sea and shortening in the Apennines as a result of arc migration driven by sinking of lithosphere. Tectonics 5, 227–245. http://dx.doi.org/10.1029/TC005i002p00227.
Mastrolembo Ventura, B., Serpelloni, E., Argnani, A., Bonforte, A., Bürgmann, R., Anzidei, M., Baldi, P., Puglisi, G., 2014. Fast geodetic strain-rates in eastern Sicily (southern Italy): New insights into block tectonics and seismic potential in the area of the great 1693 earthquake. Earth Planet. Sci. Lett. 404, 77–88. http://dx.doi.org/10.1016/j.epsl.2014.07.025.
Ministero dello Sviluppo Economico, DGS-UNMIG, 2014. Indirizzi e linee guida per il monitoraggio della sismicità, delle deformazioni del suolo e delle pressioni di poro nell'ambito delle attività antropiche. Available at http://unmig.mise.gov.it/unmig/agenda/upload/85_238.pdf (Accessed October 31, 2017).
Ministero dello Sviluppo Economico (2013). Rapporto annuale 2013, Attività dell'anno 2012. Roma, Direzione Generale per le Risorse Minerarie ed Energetiche. Available at: http://unmig.sviluppoeconomico.gov.it/unmig/stat/ra2013.pdf (Accessed October 31, 2017).
Modoni, G., Darini, G., Spacagna, R.L., Saroli, M., Russo, G., Croce, P., 2013. Spatial analysis of land subsidence induced by groundwater withdrawal. Eng. Geol. 167, 59–71. http://dx.doi.org/10.1016/j.enggeo.2013.10.014.
Montone, P., Mariucci, M.T., 2016. The new release of the Italian contemporary stress map. Geophys. J. Int. 205, 1525–1531. http://dx.doi.org/10.1093/gji/ggw100.
Musumeci, C., Scarfì, L., Palano, M., Patanè, D., 2014. Foreland segmentation along an active convergent margin: new constraints in southeastern Sicily (Italy) from seismic and geodetic observations. Tectonophysics 630, 137–149. http://dx.doi.org/10.1016/j.tecto.2014.05.017.
Palano, M., 2015. On the present-day crustal stress, strain-rate fields and mantle anisotropy pattern of Italy. Geophys. J. Int. 200 (2), 969–985. http://dx.doi.org/10.1093/gji/ggu451.
Pieri, M., Groppi, G., 1981. Subsurface geological structure of the Po plain, Italy. CNR, Progetto Finalizzato Geodinamica 414, 13.
Polcari, M., Albano, M., Saroli, M., Tolomei, C., Lancia, M., Moro, M., Stramondo, S., 2014. Subsidence detected by multi-pass differential SAR interferometry in the cassino plain (Central Italy): joint effect of geological and anthropogenic factors? Remote Sens. 6, 9676–9690. http://dx.doi.org/10.3390/rs6109676.

Pondrelli, S., Salimbeni, S., Ekström, G., Morelli, A., Gasperini, P., Vannucci, G., 2006. The Italian CMT dataset from 1977 to the present. Phys. Earth Planet. Int. 159 (3-4), 286–303. http://dx.doi.org/10.1016/j.pepi.2006.07.008.

Raspini, F., Loupasakis, C., Rozos, D., Moretti, S., 2013. Advanced interpretation of land subsidence by validating multi-interferometric SAR data: the case study of the Anthemountas basin (Northern Greece). Nat. Hazards Earth Syst. Sci. 13 (10), 2425–2440. http://dx.doi.org/10.5194/nhess-13-2425-2013.

Regione Emilia-Romagna and ENI-AGIP, 1998. In: Di Dio, G. (Ed.), Riserve idriche sotterranee della Regione Emilia-Romagna, pp. 120 (Soc. Elaborazioni Cartogr., Firenze, Italy).

Regione Emilia-Romagna-Arpa Emilia-Romagna, 2012. Rilievo della subsidenza nella pianura emiliano-romagnola, Seconda Fase. Relazione Finale.

Rovida, A., Locati, M., Camassi, R., Lolli, B., Gasperini, P., 2016. CPTI15, The 2015 Version of the Parametric Catalogue of Italian Earthquakes. Istituto Nazionale di Geofisica e Vulcanologiahttp://dx.doi.org/10.6092/INGV.IT-CPTI15.

Scrocca, D., Carminati, E., Doglioni, C., Marcantoni, D., 2007. Slab retreat and active shortening along the central-northern Apennines. In: Lacombe, O., Roure, F., Lavé, J., Vergés, J. (Eds.), Thrust Belts and Foreland Basins. Frontiers in Earth Sciences. Springer Berlin, Heidelberg.

Serpelloni, E., Anzidei, M., Baldi, P., Casula, G., Galvani, A., 2005. Crustal velocity and strain-rate fields in Italy and surrounding regions: new results from the analysis of permanent and non-permanent GPS networks. Geophys. J. Int. 161 (3), 861–880. http://dx.doi.org/10.1111/j.1365-246X.2005.02618.x.

Serpelloni, E., Faccenna, C., Spada, G., Dong, D., Williams, S.D.P., 2013. Vertical GPS ground motion rates in the Euro-Mediterranean region: new evidence of velocity gradients at different spatial scales along the Nubia-Eurasia plate boundary. J. Geophys. Res. Solid Earth 118, 6003–6024. http://dx.doi.org/10.1002/2013JB010102.

Serpelloni, E., Vannucci, G., Anderlini, L., Bennett, R.A., 2016. Kinematics, seismotectonics and seismic potential of the eastern sector of the European Alps from GPS and seismic deformation data. Tectonophysics 688, 157–181. http://dx.doi.org/10.1016/j.tecto.2016.09.026.

Stramondo, S., Saroli, M., Tolomei, C., Moro, M., Doumaz, F., Pesci, A., Boschi, E., 2007. Surface movements in bologna (Po Plain-Italy) detected by multitemporal DInSAR. Remote Sens. Environ. 110 (3), 304–316. http://dx.doi.org/10.1016/j.rse.2007.02.023.

Stramondo, S., Bozzano, F., Marra, F., Wegmuller, U., Cinti, F.R., Moro, M., Saroli, M., 2008. Subsidence induced by urbanisation in the city of Rome detected by advanced InSAR technique and geotechnical investigations. Remote Sens. Environ. 112 (6), 3160–3172. http://dx.doi.org/10.1016/j.rse.2008.03.008.

Svigkas, N., Papoutsis, I., Loupasakis, C., Tsangaratos, P., Kiratzi, A., Kontoes, C.H., 2016. Land subsidence rebound detected via multi-temporal InSAR and ground truth data in Kalochori and Sindos regions, Northern Greece. Eng Geol. 209, 175–186. http://dx.doi.org/10.1016/j.enggeo.2016.05.017.

Svigkas, N., Papoutsis, I., Loupasakis, K., Tsangaratos, P., Kiratzi, A., Kontoes, Ch., 2017. InSAR time-series monitoring of ground displacement trends in an industrial area (Oreokastro-Thessaloniki, Greece): detection of natural surface rebound and new tectonic insights. Environ. Earth Sci. 76 (5), 195. http://dx.doi.org/10.1007/s12665-017-6517-9.

Taniguchi, M., Shimada, J., Fukuda, Y., Yaman, M., Onodera, S., Kaneko, S., Yoshikoshi, A., 2009. Anthropogenic effects on the subsurface thermal and ground water environments in Osaka, Japan and Bangkok. Thailand. Sci. Total Environ. 407 (9), 3153–3164. http://dx.doi.org/10.1016/j.scitotenv.2008.06.064.

Tape, C., Musé, P., Simons, M., Dong, D., Webb, F., 2009. Multiscale estimation of GPS velocity fields. Geophys. J. Int. 179, 945–971. http://dx.doi.org/10.1111/j.1365-246X.2009.04337.x.

Teatini, P., Ferronato, M., Gambolati, G., Bertoni, W., Gonella, M., 2005. A century of land subsidence in Ravenna. Italy. Environ. Geol. 47 (6), 831–846. http://dx.doi.org/10.1007/s00254-004-1215-9.

Teatini, P., Ferronato, M., Gambolati, G., Gonella, M., 2006. Groundwater pumping and land subsidence in the Emilia-Romagna coastland, Italy: modeling the past occurrence and the future trend. Water Resour. Res. 42, W01406. http://dx.doi.org/10.1029/2005WR004242.

Vollrath, A., Zucca, F., Bekaert, D., Bonforte, A., Guglielmino, F., Hooper, A.J., Stramondo, S., 2017. Decomposing DInSAR time-series into 3-D in combination with GPS in the case of low strain rates: an application to the hyblean plateau, sicily. Italy. Remote Sens. 9 (1), 33. http://dx.doi.org/10.3390/rs9010033.

Zebker, H.A., Rosen, P.A., Goldstein, R.M., Gabriel, A., Werner, C.L., 1994. On the derivation of coseismic displacement fields using differential radar interferometry: the Landers earthquake. J. Geophys. Res. 99 (B10), 19617–19634. http://dx.doi.org/10.1029/94JB01179.

Zhou, X., Chang, N.B., Li, S., 2009. Applications of SAR interferometry in earth and environmental science research. Sensors 9, 1876–1912. http://dx.doi.org/10.3390/s90301876.